Characterization of a Thermoset by Thermal Analysis Techniques: Criterion To Assign the Value of the α-Transition Temperature by Dielectric Analysis

Lisardo Núñez-Regueira, C. A. Gracia-Fernández, S. Gómez-Barreiro

Research Group Terbipromat, Departamento Física Aplicada, Universidade de Santiago 15782, Santiago, Spain

Received 9 June 2004; accepted 18 October 2004
DOI 10.1002/app.21657
Published online in Wiley InterScience (www.interscience.wiley.com).

ABSTRACT: A cured thermoset composed of diglycidyl ether of bisphenol A and *m*-xylylene diamine as the cure agent was studied with different thermal analysis techniques, including differential scanning calorimetry (DSC), dynamic mechanical analysis (DMA), and dielectric analysis (DEA). DSC was used to measure the glass-transition temperature and to check the absence of the heat of reaction. DMA and DEA were used to show the existence of two transitions in the temperature range of −100 to 240°C. The transition at a low temperature corresponded to the β transition. The second one, at a higher temperature, was associated with an α transition. The β transition followed Arrhenius behavior, whereas the α transition followed Vogel behavior. For an analysis of the α transition, different equations, such as the Havriliak–Negami, Vogel, and Williams–Landel–Ferry equations, were used. Important differences related to the fitting parameters were found that depended on the type of equation and the operation mode used. For this reason, a new method for calculating the α-transition temperature was examined. © 2005 Wiley Periodicals, Inc. J Appl Polym Sci 96: 2027–2037, 2005

Key words: dielectric properties; glass transition; mechanical properties; relaxation

INTRODUCTION

Thermoset materials, including those derived from epoxy resins, have been widely[1–6] studied both during the curing process and as cured materials. It is widely recognized that the relaxation time of a polymeric material is one of the main parameters for characterization. However, as far as we know, little has been done to determine the influence of the methods used to obtain the relaxation times on the results subsequently obtained through the different models used for cured thermosets.

In our case, the relaxation times have been mainly determined with dielectric analysis (DEA) because it allows the use of a very wide range of frequencies. This thermal analysis technique is a perfect complement to other different techniques of thermal analysis[7] because it identifies the transitions from the electrical properties of the materials.

Using the obtained relaxation times, we propose a criterion for determining the α-transition temperature (T_α) that is independent of the operation mode (isothermal or dynamic).

This study was carried out with the epoxy system diglycidyl ether of bisphenol A (DGEBA; $n = 0$)/*m*-xylylene diamine (*m*-XDA). The curing agent was because of the ease with which it forms high-density three-dimensional networks. This ease is based on the capacity of its aromatic carbon to rotate freely in space.

Theoretical background

One of the main characteristics of epoxy polymers is their viscoelasticity; consequently, their behavior is somewhere between that of an elastic solid and that of an ideal viscous liquid. It is well known that the energy applied to an elastic solid is stored in it as potential energy and can, therefore, be recovered. Moreover, some of the energy supplied to a viscous liquid is lost as heat or some other form of dissipated energy. Important information about the viscoelastic behavior of epoxy resin materials can be obtained by the study of the responses of these materials to periodic forces. The strain (E) can be varied sinusoidally as follows:

$$E = E_0 \cos \omega t \quad (1)$$

where E_0 is the maximum amplitude of the strain, ω is the frequency, and t is the time.

The stress (σ) may be given by[8]

Correspondence to: L. Núñez-Regueira (falisar1@usc.es).
Contract grant sponsor: Secretaria Xeral de Investigación e Desenvolvemento (Xunta de Galicia).

Journal of Applied Polymer Science, Vol. 96, 2027–2037 (2005)

$$\sigma = \sigma_0 \cos(\omega t + \delta) = \sigma_0(\cos\omega t \cos\delta - \sin\omega t \sin\delta) \quad (2)$$

where σ_0 is the amplitude of the stress and

$$E' = \left(\frac{\sigma_0}{\varepsilon_0}\right)\cos\delta \quad \text{and} \quad E'' = \left(\frac{\sigma_0}{\varepsilon_0}\right)\sin\delta \quad (3)$$

with a quotient

$$\tan\delta = \frac{E''}{E'} \quad (4)$$

which is called the loss tangent. It relates the dissipated and stored energies in every cycle. E' and E'' are the storage and loss moduli corresponding either to DSC or DEA experiments, respectively, and ε_0 is the permittivity of the free space.

For highly crosslinked polymers, in the transition zone between glass and rubberlike consistency, both E'' and the loss tangent pass through a pronounced maximum.

For dielectric measurements, the complex dielectric constant (ε^*) of a material can be separated into its real and imaginary parts: ε' is the relative permittivity (real), and ε'' is the relative loss factor (imaginary). Both are related to ε_0 (equal to 8.85×10^{-12} F m^{-1}):

$$\varepsilon^* = \varepsilon' - i\varepsilon'' \quad (5)$$

Both ε' and ε'' depend on the measurement frequency. The ratio $\varepsilon''/\varepsilon'$ is known as the dissipation or loss tangent:

$$\tan\delta = \frac{\varepsilon''}{\varepsilon'} \quad (6)$$

where δ is the phase angle between the input voltage and the output current.

It is well known[9–17] that when a material is subjected to an applied electric field, the dipoles in the material will orient in the direction of the electric field. The orientation involves a characteristic time, called the dipole relaxation time (τ_d).

ε' is low when the measurements are carried out at low temperatures because the molecules are immobilized at their positions, and this prevents the dipoles from orienting in the direction of the electric field. For the same reason, ε' is low in highly crosslinked resins.

ε'' measures the energy required for molecular motion in the presence of an electric field. It involves two contributions: energy losses due to the orientation of molecular dipoles and energy losses due to the conduction of ionic species. The conduction process arises only at temperatures well above the glass-transition temperature (T_g), as measured by differential scanning calorimetry (DSC) for this epoxy system.

We use the Havriliak–Negami (H–N)[18,19] equation to analyze the data presented in this article:

$$\varepsilon^* = \varepsilon_r + \frac{\varepsilon_r - \varepsilon_u}{[1 + (iw\tau_d)^{1-a}]^b} \quad (7)$$

where ε_u is the unrelaxed permittivity; ε_r is the relaxed permittivity; ω is the angular frequency; and a and b are parameters ($0 < a < 1$, $0 < b < 1$) describing the symmetric and asymmetric broadening of the relaxation time distribution, respectively.

To fit experimental data to eq. (7), we separated ε^* into its real and imaginary parts.

In the domain of temperatures, according to the type of transition, the Arrhenius [eq. (8)] and Vogel[20] [eq. (9)] equations were used:

$$\omega = \omega_0 e^{-E_a/RT} \quad (8)$$

$$\omega = Ae^{-B/T-T_0} \quad (9)$$

where ω_0 is the reference frequency, E_a is the apparent activation energy of the process, A and B are experimental parameters, T_0 is the so-called Vogel temperature, T is the temperature (K), and R is the gas constant.

Williams et al.[21] proposed an empirical relationship describing the dependence on the temperatures of the relaxation times (or their frequency equivalents) in the glass-transition region. This equation is known as the Williams–Landel–Ferry (WLF) equation and is generally written as follows:

$$\log a_T = \log\frac{\tau(T)}{\tau(T_S)} = -\log\frac{\omega}{\omega_S} = \frac{-C_1(T - T_S)}{C_2 + (T - T_S)} \quad (10)$$

where a_T is the ratio of the relaxation time at temperature T to the relaxation time at a reference temperature T_S, τ is the relaxation time, ω_S is the angular frequency at temperature T_S, and C_1 and C_2 are constants that depend, among other things, on the value chosen for T_S. In this article, T_S is taken to be the T_g value measured by DSC. Equation (10) was found to apply in the temperature range from T_g to about T_g + 100°C.

EXPERIMENTAL

Materials

The epoxy resin was DGEBA ($n = 0$; Resin 332, Sigma Chemical Co., St. Louis, MO) with an epoxy equivalent between 172 and 176. The curing agent was *m*-XDA (99%; Aldrich, Switzerland). It was used as received.

The resin and diamine were carefully and homogeneously mixed in a stoichiometric ratio of 100:18. Once

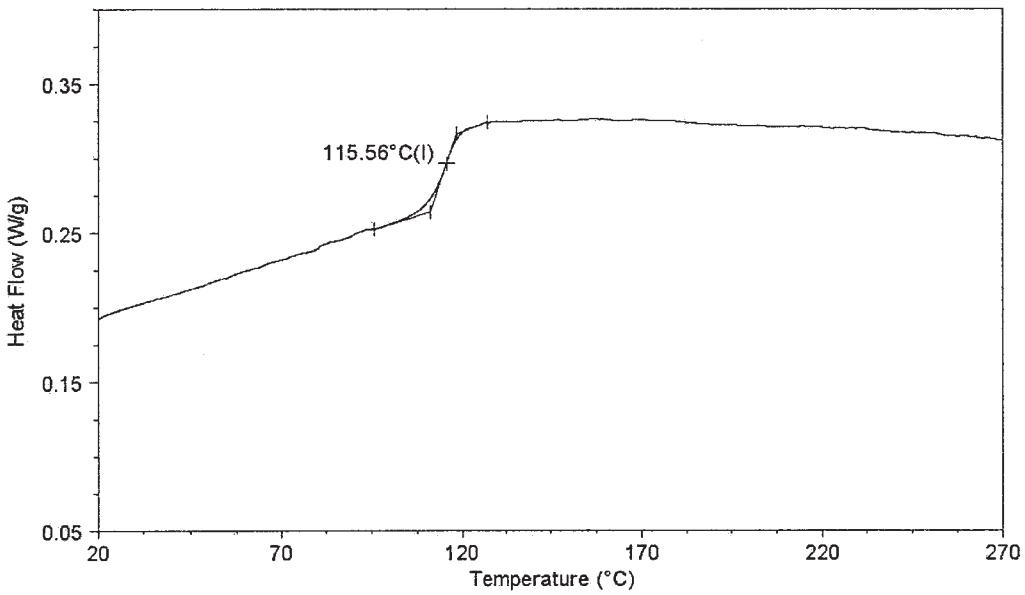

Figure 1 Heat flow versus the temperature for the cured DGEBA/*m*-XDA system.

mixed, the sample was added to a frame to cure. The frame consisted of two steel plates covered by two smooth Teflon sheets and a Teflon pattern with 20 holes (2.5 cm × 2.5 cm × 0.5 cm thick).

The curing of the systems was achieved according to a time–temperature–transformation (TTT) diagram previously designed[22] for this epoxy system. It consisted of two steps: a first step of 20 min at 40 °C followed by a second one for 2 h 28 min at 200 °C.

DSC

DSC measurements were performed with a TA Instruments Modulated DSC 2920 instrument (New Castle, DE) with a helium DSC cell purge (at 25 mL/min). Hermetic aluminum pans were used. The instrument was calibrated for the temperature with cyclohexane and indium.

Dynamic mechanical analysis (DMA)

The viscoelastic properties were measured with a Polymer Laboratories MK II dynamic mechanical thermal analyzer (Aldrich, Switzerland) working in the tensile mode. The real and imaginary components of the modulus of the samples were determined at 1, 3, 10, and 30 Hz.

DEA

Dielectric measurements were carried out with a DEA 2970 dielectric analyzer from TA Instruments. The measurement assembly was a parallel-plate structure.

The sensors had to be calibrated for every experiment. They used a geometrical value derived from the response of the electrode plate surface (mm^2) and the platinum resistance temperature detector (RTD) value corresponding to the resistance at 0°C observed by the platinum thermometer in the base sensor.

Each sample was under a maximum strength of 250 N to ensure good contact between the sample and the electrodes below T_g, and the heating rate was 2°C/min. The minimum space between the top and bottom electrodes was, according to the manual and the maximum force, 0.501 mm; this prevented soft samples from being squeezed out of the sensor area during an experiment. All the experiments were carried out under a dry nitrogen atmosphere at a gas flow rate of 0.5 mL min^{-1}.

RESULTS AND DISCUSSION

The first step in this research was the evaluation of T_g of the system by DSC. The temperature of the samples was controlled from −8 to 250°C at a heating rate of 10°C/min; this resulted in the curve shown in Figure 1. T_g was determined as the temperature corresponding to the inflexion point of the curve (115°C). Moreover, there was no residual heat of reaction, and this ensured a high degree of reaction.

In a previous article,[23] this same epoxy system was studied in our laboratories by DMA with a stress sinusoidal test. The study was focused on the glass transition. T_g was taken as the temperature corresponding to the maximum of the tan δ/temperature curve at a frequency of 1 Hz. This study widens the lower temperature limit from 30 to −145°C. Moreover, for comparison, the DEA technique was used from

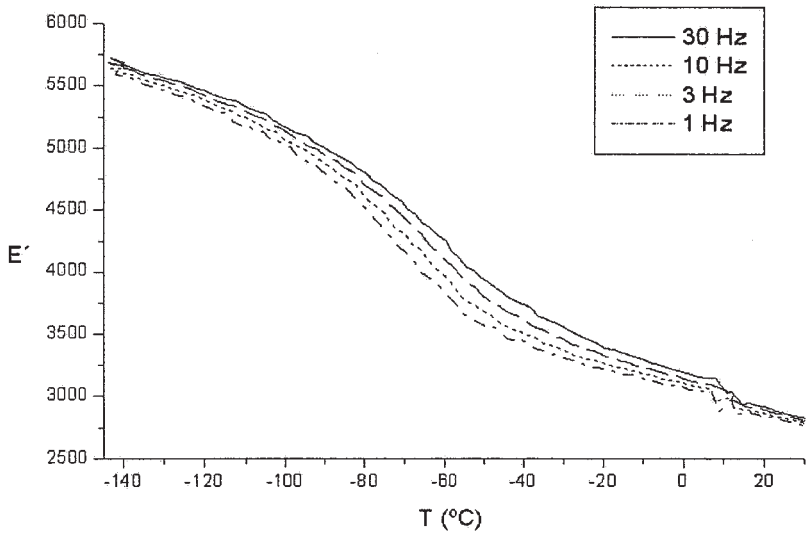

(a)

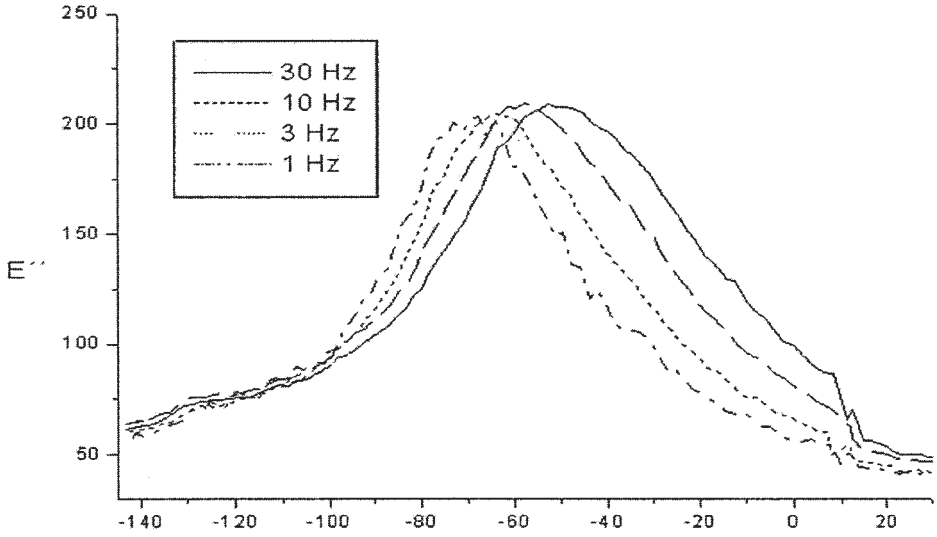

(b)

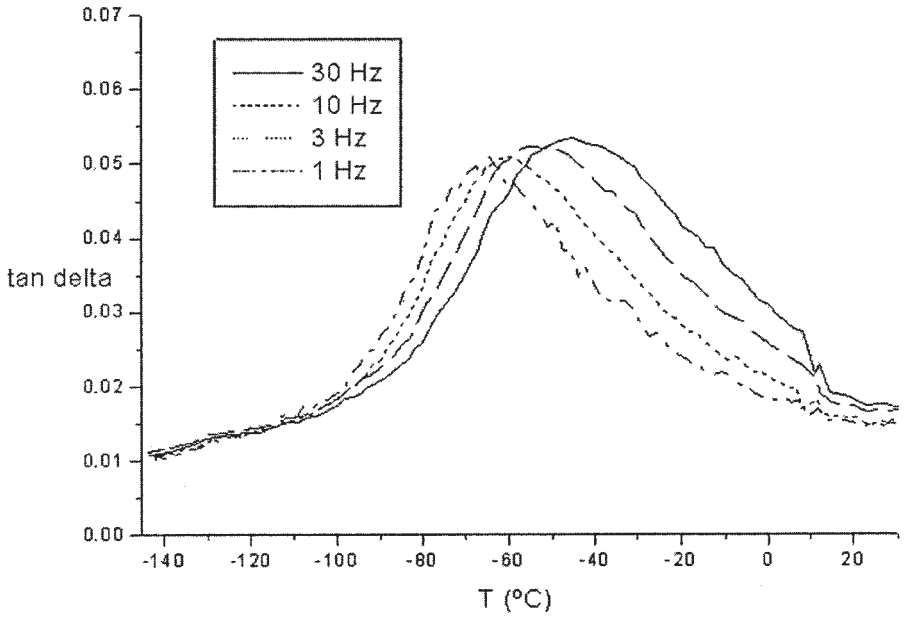

(c)

Figure 2 (a) E', (b) E'', and (c) tan δ versus the temperature (°C) for the cured DGEBA/*m*-XDA system.

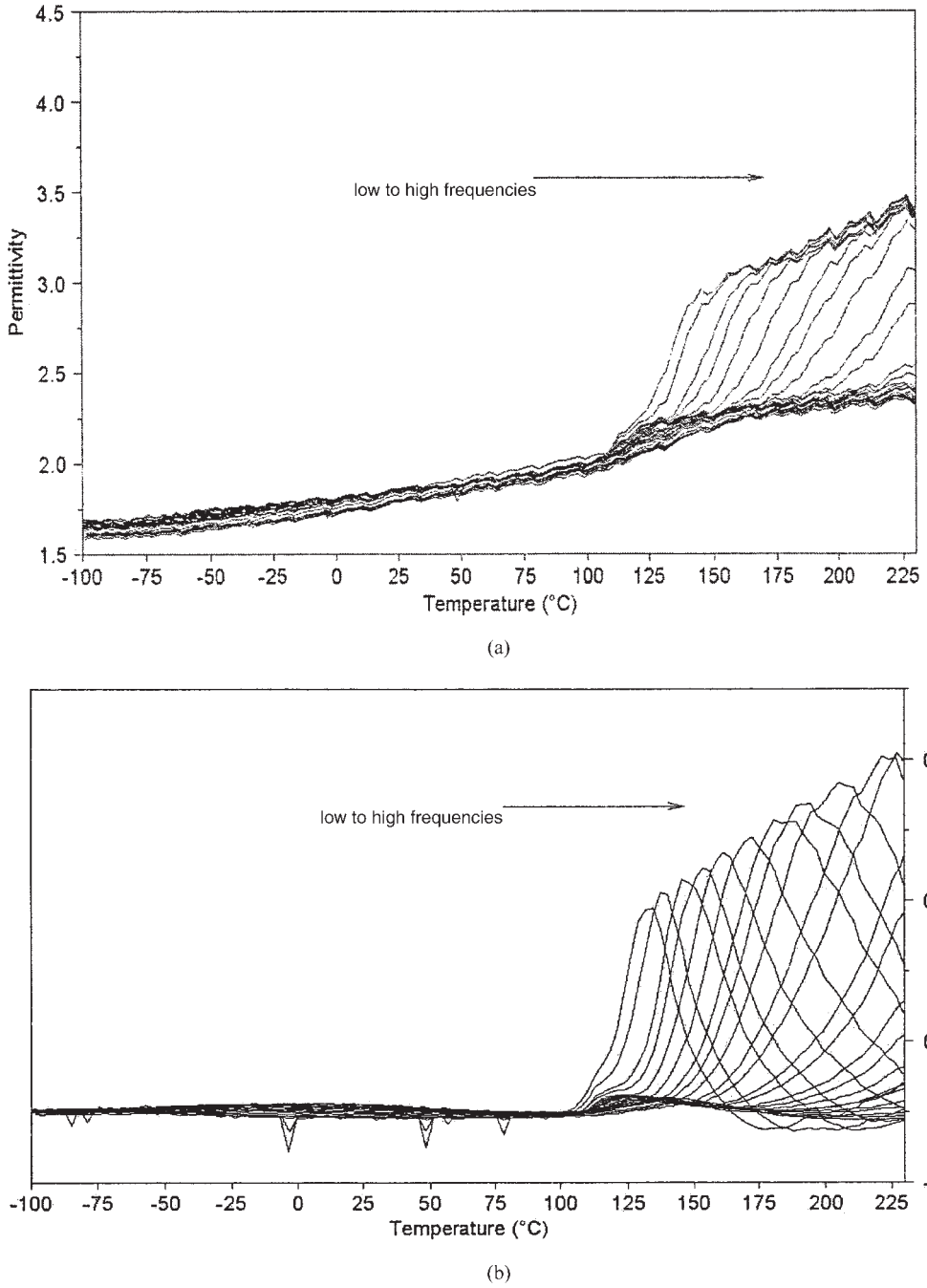

Figure 3 (a) ε' and (b) ε'' versus the temperature (°C) for the cured DGEBA/*m*-XDA system.

−100 to 220°C. The choice of the upper limit was necessary because we used the WLF equation valid from T_g to T_g + 100°C. Furthermore, by doing so, we ensured the nonexistence of conductivity or polarization phenomena that could overlap our dipole relaxation measurements.

Figure 2(a–c) shows DMA measurements at frequencies of 1, 3, 10, and 30 Hz from −145 to 30°C. As expected for typical thermoset behavior,[24] E' decreased with increasing temperature, whereas E'' and tan δ showed peaks associated with the E' decrease. The observed transition corresponded to a β transition related to side-chain motions. This kind of behavior has been reported in the literature for the system used in this research.[25]

Figure 3(a,b) shows ε' and ε'', respectively, as functions of the temperature at a heating rate of 2°C/min (dynamic measurements). The frequency range was 1×10^{-1} to 1×10^{5} Hz. This range of 6 decades allowed a wide characterization of the β transition. For the α transition, because of the temperature range studied, only frequencies up to 200 Hz were necessary.

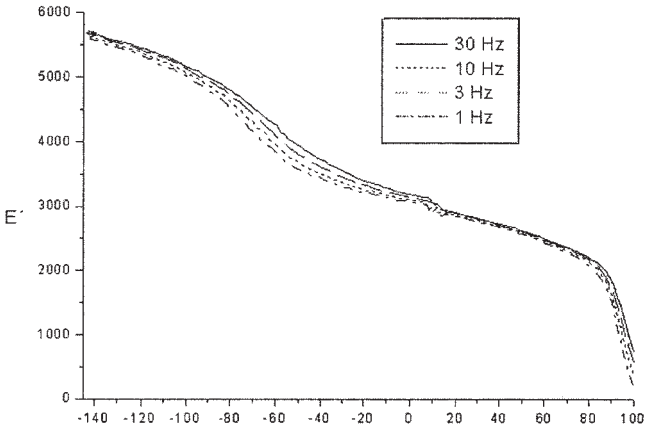

Figure 4 E' versus the temperature (°C) for the cured DGEBA/*m*-XDA system (wide range).

Figure 3(a) is a plot of ε' as a function of temperature at different frequencies; the α transition can be clearly observed as a sharp increase in ε' as a result of the dipole contribution. However, the β transition can hardly be observed.

The behavior of ε'' as a function of temperature at different frequencies is shown in Figure 3(b). Again, a great difference between the α and β transitions is observed.

The β-transition temperature (T_β) and the α-transition temperature ($T_\alpha = T_g$ by DSC) were taken as those temperature corresponding to the ε'' maximum at each frequency.

To better determine the difference between the two transitions, we widened the experimental temperature range used in a previous DMA study for this epoxy system. The results are presented in Figure 4, in which E' is plotted as a function of temperature at frequencies of 1, 3, 10, and 30 Hz. In this case, the difference between the two transitions was much smaller than that of the dielectric measurements. This meant that the β transition involved greater changes in the mechanical properties than in the dielectric properties. This could be a result of the low values of the dipole moments of the chains involved in this transition.

For a comparison of the mechanical and dielectric data, the values of T_g or T_α were taken as those corresponding to the maximum of tan δ at 1 Hz (DMA) and as those corresponding to the maximum of ε'' at 0.1 Hz (DEA) according to a study by Núñez et al.[26] A very good agreement was found, with values of 122 (DEA) and 123.1°C (DMA). The same criterion was used for T_β, and the results were −77 and −66.7°C for DEA and DMA, respectively. These values were in good agreement with those previously reported.[25]

Figure 5(a) shows a plot of ln f versus $1000/T$ corresponding to the β-transition values of our epoxy system as measured by DMA and DEA. The experimental data followed an Arrhenius-like behavior, and this allowed the calculation of E_a. According to the DMA data, E_a was 64 kJ/mol, whereas according to the DEA data, E_a was 59.6 kJ/mol, in good agreement with the values calculated by Matsukawa et al.[24] for a cured epoxy system.

Dielectric measurements

An Arrhenius plot for the α and β relaxations is shown in Figure 5(b). Although the β relaxation followed an Arrhenius behavior, the α relaxation followed a Vogel-like behavior typical of these types of systems. Because of this, the experimental data corresponding to the α transition were fitted to the Vogel and WLF equations. The reference temperature was taken as that corresponding to T_g as measured by DSC. The values of the different parameters obtained with the aforementioned equations are listed in Table I.

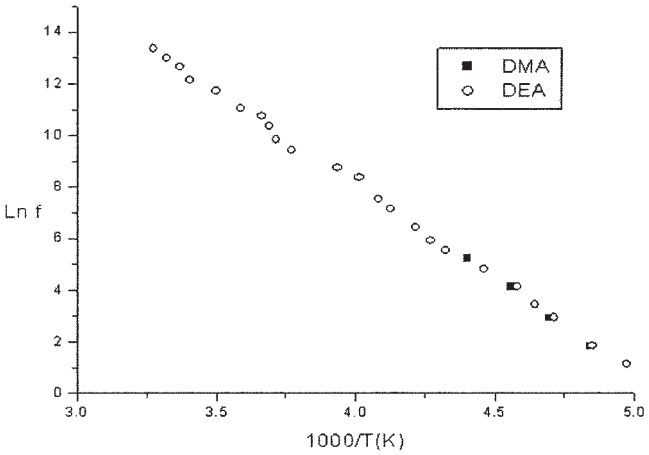

(a)

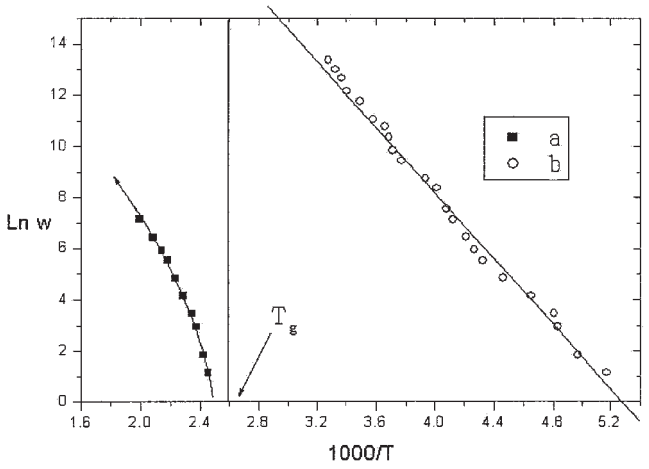

(b)

Figure 5 Arrhenius plots of (a) the β transition measured by DEA and DMA and (b) the β and α transitions measured by DEA.

TABLE I
Parameters of the Vogel and WLF Equations

	Dynamic (dm)	Isothermal (im)	dynamic (dvm)	Isothermal (idm)	H–N
A	13,648.83	10,639.61	11,632.42	12,612.23	1738.86
B	652	520.66	714.14	729.01322	461.64
T_0	345	343.38	332.20	331.50	351.48
C_1	6.23574	5.63	6.52	6.58	5.48
C_2	53.87283	58.06	83.94	83.05	34.85
ω_S	0.32	0.16	0.20	0.18	0.05

For the α transition, our basic objective was to find relationships between the relaxation times (or frequencies) and other physical parameters obtained by DEA in the dynamic or isothermal modes and also with different transition theories. With this aim, we performed a study from 134 to 174°C, that is, above T_g (rubber state) and below temperatures that could overlap conductivity with dipole relaxation (our objective). We carried out the isothermal experiments by increasing the temperature in 4°C steps and keeping each temperature constant for 5 min; this allowed frequency scans from 0.5 to 10^4 Hz at each temperature. By doing so, we ensured that all the frequencies were measured at the same temperatures, as a frequency scan took around 1 min. This procedure allowed us to plot ε' and ε'' as functions of the frequency at fixed temperatures. The reason for avoiding conductivity in this study was to allow the correct use of the H–N equation. Figure 6(a) shows the frequency variation of the permittivity at different temperatures of the cured thermoset. It shows a decrease in ε' with increasing frequency. At a given temperature, the dipoles were able to follow an oscillating electric field more easily at a low frequency than at a high frequency. Thus, at a higher frequency, the dipoles did not have enough mobility to oscillate with the electric field and did not contribute to ε'. As the temperature increased, the dipoles gained mobility because of the decrease in viscosity, and then the mobility dramatically decreased.

Figure 6(b) shows the frequency variation of ε'' at a fixed temperature. All the curves present a maximum that shifts toward increasing frequencies as the temperature increases. Each ε'' maximum coincides roughly with the inflexion points of the plots of ε' versus ln ω.

Two very important parameters for dielectric relaxations are ε_r and ε_u. ε_r is the permittivity when the frequency tends to zero (low frequencies). In this case, the dipole mobility depends only on the temperature and is frequency independent. ε_r is due to electronic and atomic polarization plus static dipole polarization or orientation. ε_u is the permittivity of the system at high frequencies, ideally at an infinite frequency; it corresponds to electronic and atomic polarizations and is independent of the frequency at low frequencies.

The difference, $\Delta\varepsilon = \varepsilon_r - \varepsilon_u$, is known as the dipole strength and represents the contribution to the real part of permittivity of the dipoles in the system. As previously mentioned, an Argand diagram shows the frequency dependence of ε' and ε''; ε' is plotted against ε'', with ω used as a parameter. Figure 7 shows this diagram. As the observed Argand diagrams differ from ideal ones, in this study we have used for dis-

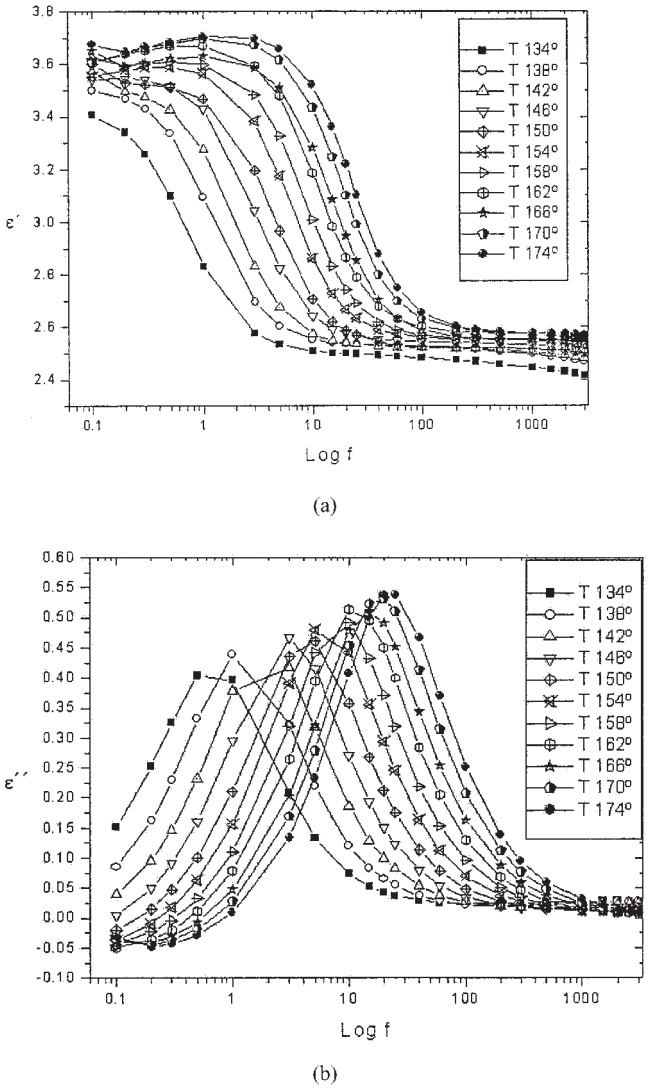

Figure 6 (a) ε' and (b) ε'' versus log f for the cured DGEBA/*m*-XDA system.

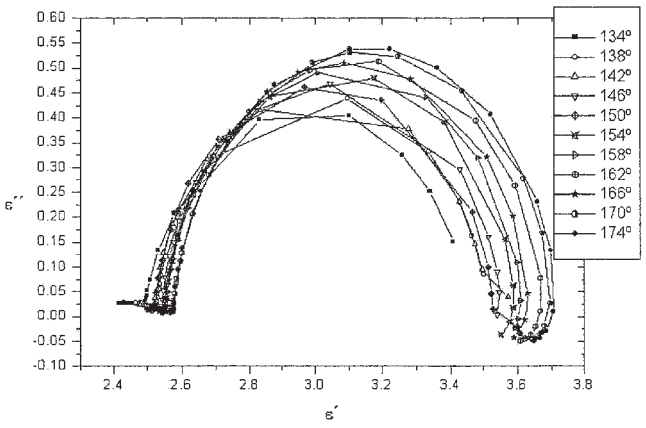

Figure 7 Argand plot of the α transition of the cured DGEBA/*m*-XDA system.

cussion the method proposed by Havriliak and Negami.[18,19]

With this aim, the H–N equation was divided into its real and imaginary parts, which were used separately to model ε' and ε'', as functions of the frequency. By doing so, we obtained values of ε_r, ε_u, $\Delta\varepsilon$, τ, a, and b. To increase this information, we plotted all these parameters as temperature functions. Figure 8 shows plots of ε_r, ε_u, and $\Delta\varepsilon$ versus the temperature. Each of these parameters remained practically constant within the temperature range used for our study. The fact that ε_u remained constant meant that electronic and atomic polarizability did not change with the temperature within the experimental temperature range considered here.

To analyze the constancy of ε_r and $\Delta\varepsilon$, we had to consider that the oscillator strength depended on various factors, such as the temperature, network parameters and intramolecular interactions, and polarizability of the system. For this reason, the fact that ε_r and $\Delta\varepsilon$ remained constant meant that the influence of all these factors was cancelled among them.

As previously mentioned, parameter a in eq. (7) describes the symmetrical broadening of the relaxation time distribution associated with any molecular relaxation (in our case, a dipole one), whereas b accounts for the asymmetrical behavior of the mathematical function. Both have values of 0–1. $a = 0$ represents a distribution with a relaxation time according to the ideal Debye model. When a is 1, the function presents its maximum width. $b = 1$ also corresponds to a completely symmetrical distribution function, as predicted by the Debye model, that tends to asymmetry as b approaches 0.

Figure 9(a) shows a as a function of the temperature within the range used for our study. a is very close to zero in the whole range studied, and this indicates a very narrow relaxation time function or, in other words, the existence of a dominant dipole species. The fact that a decreases with an increase in the temperature also indicates the reduction of the distribution broadening, and this means that this dipole becomes more dominant.

Figure 9(b) is a plot of b versus temperature. Again, the distribution function is a symmetric one because b is always very close to 1.

The values of a and b indicate that the relaxation time function is rather symmetric, and this suggests that both the mean and maximum values of the relaxation time function are very similar as a result of the very narrow representative curve. Again, this fact indicates the existence of a strongly dominant dipole for the relaxation time distribution. The fact that both the mean relaxation time and the maximum of the relaxation time function have very similar but not equal values will be helpful for a discussion of Arrhenius plots later.

The last step in this study was the analysis of the relaxation time obtained through the H–N equation. With this aim, the calculus of the frequency (f) related to the relaxation time was obtained with the following relationship:

$$\omega = 2\frac{\pi}{\tau} \quad \text{and} \quad f = \frac{1}{\tau} \tag{11}$$

In this way, the frequency associated with a given temperature can be calculated from the relaxation time.

The knowledge of the different isothermal temperatures and the frequency associated with each of them allows an analysis similar to that developed for the dynamic test. For this kind of analysis, the Vogel and WLF equations were used. The different parameters obtained are listed in Table I.

There is one other aspect to be considered from an observation of ε''–temperature plots. Figure 3 shows

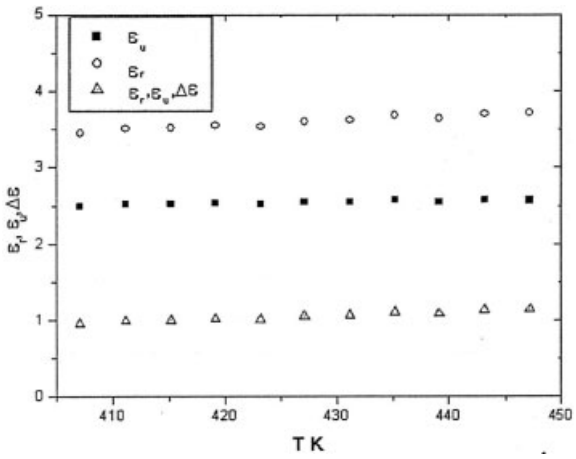

Figure 8 ε_r, ε_u, and $\Delta\varepsilon$ versus the temperature (K) for the cured DGEBA/*m*-XDA system.

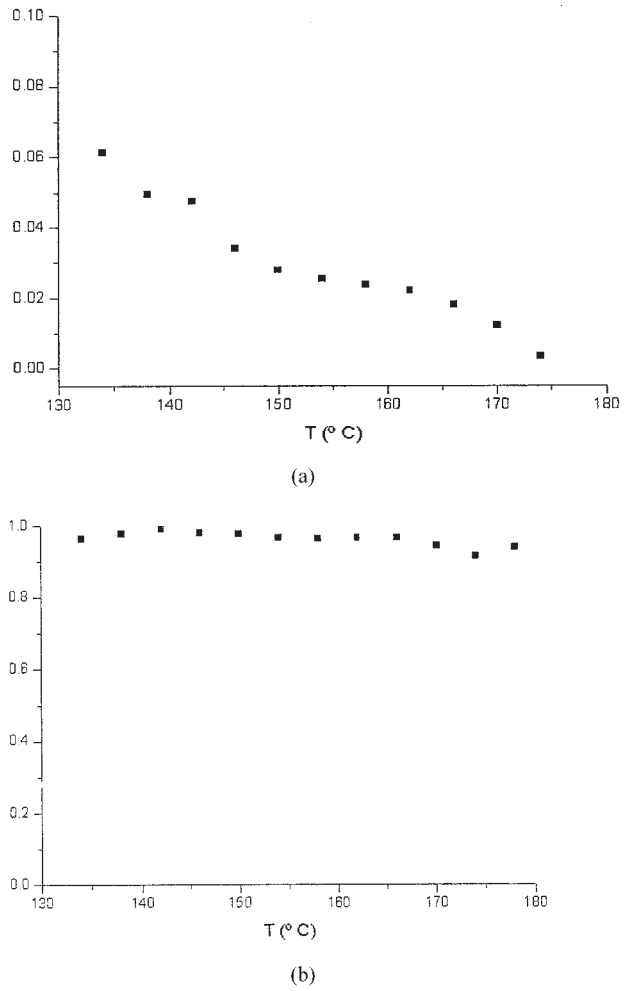

Figure 9 Plots of (a) parameter *a* and (b) parameter *b* (in the H–N equation) versus the temperature for the DGEBA/*m*-XDA system.

that these curves are asymmetric. This can be attributed to the fact that as the temperature increases, there is a change in the relaxation time distribution function and, because of that, in the relaxation behavior of the system. This asymmetry is responsible for the temperature associated with the maximum value of ε'' not coinciding with the mean value of ε'' calculated from a ε''–temperature plot. To obtain this mean value of the function $\varepsilon''(T)$, it is necessary to integrate the representative curve by numerical methods. By doing so, the temperature that divides the curve into two fifty–fifty left and right parts can be obtained. To compare isothermal and dynamic experiments, we constructed a curve of ε'' versus the temperature from isothermal data. To do this, we fixed the values of the frequency, and the values of ε'' corresponding to every isothermal experiment were measured and then presented. T_{im} is the temperature corresponding to the maximum value of ε'' at each frequency. T_{imv} is the temperature mean value obtained by the numerical integration of ε''–temperature curves at each frequency. The mean values obtained for the temperature, frequency, and relaxation time are labeled T_{dmv}, f_{dmv}, and τ_{dmv} (where dmv means dynamic mean value) and T_{imv}, f_{imv}, and τ_{imv} (where imv means isothermal mean value) for the dynamic and isothermal experiments, respectively.

These values were obtained with the objective of checking the agreement between the calculations carried out with the two methods and those obtained by the traditional method (values corresponding to the maximum of the ε''–temperature plot).

In summary, we have studied the glass transition of the epoxy system DGEBA ($n = 0$)/*m*-XDA, measuring either frequencies or relaxation times and the temperatures with five different methods. All these values are recorded in Table II.

For the dynamic experiments, in the first step, we measured the temperature at which ε'' achieved its maximum value, at each frequency, in an ε''–temperature plot (T_{dm}, f_{dm}, and τ_{dm}, where dm means dynamic maximum). In a second step, the temperature was calculated that divided the ε''–temperature plot into two parts of equal surface area at each frequency (T_{dmv}, f_{dmv}, and τ_{dmv}).

For the isothermal experiments, we followed the same procedure used for the dynamic experiments, obtaining T_{im}, f_{im}, and τ_{im} and T_{imv}, f_{imv}, and τ_{imv} for the maximum and mean values, respectively. Moreover, in this case, the relaxation times were fitted to the H–N equation, and T_{H-N}, f_{H-N}, and τ_{H-N} were obtained.

Once all the aforementioned values were obtained for the dynamic and isothermal experiments, we began our analysis. In the first place, values corresponding to the maximum of the ε'' function (T_{dmv}, f_{dmv}, and τ_{dmv} and T_{im}, f_{im}, and τ_{im}) were compared. With this aim, a plot of $T_{dm} - T_{im}$ as a function of the relaxation time, at a given frequency, was constructed (Fig. 10).

This figure shows that as the temperature increased and the relaxation time decreased, $T_{dm} - T_{im}$ increased, and this difference became positive for $\tau \leq 0.2$ s. This indicated a change in the system behavior that depended on the type of experiment. In a second analysis, data corresponding to the mean values of the dynamic and isothermal experiments (T_{dmv}, f_{dmv}, and τ_{dmv} and T_{imv}, f_{imv}, and τ_{imv}, respectively) were compared. Table II shows that these values were very close, with a difference of less than 0.1°C. This means that the values of the α-relaxation time obtained through the isothermal and dynamic experiments were practically the same.

The difference $T_{dm} - T_{im}$ increased with the frequency or with the temperature.

Figure 11 shows that, in all cases, plots of ln ω versus $1000/T$ followed a Vogel-like behavior.

Because of this, eq. (9) was used to fit experimental data (temperature and relaxation times). The values obtained for the different fitting parameters are shown

TABLE II
Values of the Temperatures and Frequencies Obtained in Five Different Ways for the Cured DGEBA/*m*-XDA System

T_{H-N}	f_{H-N}	T_{dm}	f_{dm}	T_{im}	f_{im}	T_{dvm}	f_{dvm}	T_{ivm}	f_{ivm}
407.15	0.66836	407.48	0.5	395.15	0.1	406.95	0.5	396.15	0.1
411.15	1.16362	412.99	1	399.15	0.2	413.15	1	400.45	0.2
415.15	1.90237	421.15	3	401.15	0.3	424.35	3	403.05	0.3
419.15	2.89519	426.48	5	405.15	0.5	430.95	5	406.85	0.5
423.15	4.26112	437.55	10	411.15	1	440.05	10	412.75	1
427.15	5.93331	448.35	20	421.15	3	451.25	20	425.45	3
431.15	8.14133	459.17	40	427.15	5	465.05	40	431.65	5
435.15	10.79914	467.36	60	437.15	10	472.65	60	440.55	10
439.15	14.19446	480.81	100	447.15	15	485.15	100	446.95	15
443.15	17.34605	502.43	200	451.15	20			452.05	20
447.15	20.85071	510.53	300	453.15	25			456.05	25
451.15	25.79979	533.16	700	467.15	40			464.45	40
455.15	30.40438	542.7	1,000	473.15	60			472.95	60
493.15	178.89088	559.02	2,000	487.15	100			483.45	100
		566.97	3,000						
		575.02	5,000						
		581.11	7,500						
		583.15	10,000						
		591.34	20,000						
		596.86	30,000						
		599.76	50,000						

in Table I. An analysis of this table shows that T_0 was in all cases 30–60°C above T_g as measured by DSC. Moreover, there was relative agreement between the values of the fitting parameters corresponding to the dynamic and isothermal experiments obtained from T_α, as determined with the maximum of the $\varepsilon''(T)$–temperature plot (columns 1 and 2), or from the function $\varepsilon''(T)$ (columns 3 and 4). In the last case, the difference in T_0 was less than 1°C, whereas in the first case it was around 2°C. Again, the values corresponding to parameters A and B of the Vogel equation were in closer agreement when they were calculated from numerical integration data. The differences between the dynamic and isothermal experiments were 8% for A and 2% for B. These same parameters differed by 22 and 20%, respectively, from data corresponding to the maximum of the ε''–temperature plot. This shows once again that the best way of presenting a thermoset T_α is to use the values obtained by the numerical integration of ε'' versus the temperature. The obtained values are practically independent of the type (dynamic or isothermal) of experiment.

The values of the Vogel equation fitting parameters obtained from data calculated through the H–N equation were quantitatively different from those obtained with the methods previously described here. In particular, B was lower, and T_0 was greater, than those values obtained by the previous methods; T_0 was only 37°C lower than T_g calculated by DSC. The relaxation

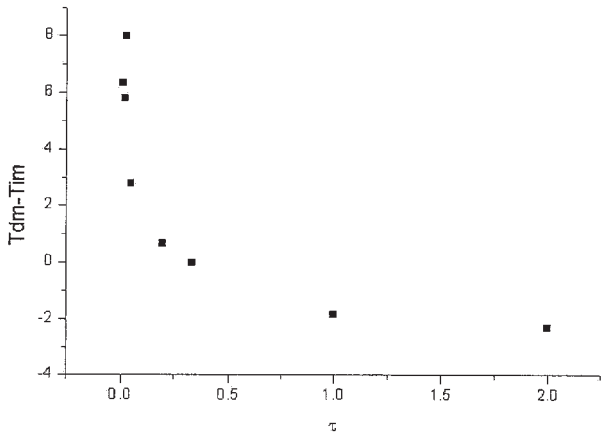

Figure 10 $T_{dm} - T_{im}$ versus τ for the cured DGEBA/*m*-XDA system.

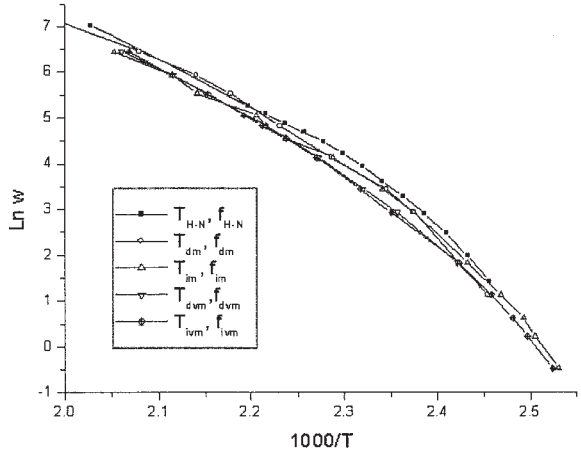

Figure 11 Arrhenius plot of the α transition for the cured DGEBA/*m*-XDA system with five kinds of data.

time obtained with the H–N equation did not correspond to the maximum of the distribution function or to its mean value.

The WLF equation [eq. (10)] was used to fit the five types of data recorded in Table II; the fitting parameters C_1, C_2, and ω_S corresponding to each case were obtained. The reference temperature was T_g determined by DSC. Table II shows the different C_1, C_2, and ω_S values. Once more, the parameters obtained by numerical integration for the dynamic and isothermal experiments were in close agreement (1% for C_1 and C_2 and 9% for ω_S).

In our opinion, this suggests the use of numerical integration to assign the temperature, frequency, and relaxation time for the α transition of a thermoset system, and it also suggests that the mean values must be calculated with consideration given to the whole loss factor curve.

Moreover, there was a great difference between the values corresponding to the maximum of the ε''–temperature plot and those corresponding to the mean value obtained from the numerical integration of the whole ε''–temperature curve. This fact suggests the inappropriate use of the WLF equation for the this system.

The last column in Table I shows values of the fitting parameters corresponding to the H–N equation. C_1 had a value similar to those obtained with previous methods. However, $C_2 = T_g - T_0$ was much lower as a result of $T_0 = 351$ K. Moreover, the frequency obtained from the H–N equation was about 4–6 times lower than that obtained with the four previous methods and thus approached a frequency zero value corresponding to a static electric field.

CONCLUSIONS

A study of the cured epoxy system DGEBA ($n = 0$)/*m*-XDA was carried out with different thermal analysis techniques.

The objective was to compare data obtained with different models existing in the literature with those measured by different techniques. It was important that the cured material had no residual heat of reaction. This was checked with DSC, which also allowed the calculation of T_g. At the same time, the reliability of DEA measurements as a function of either frequency or temperature was checked through complementary DMA measurements.

DMA was found to be more sensitive than DEA for the study of the β transition. The H–N equation was used to fit the α-relaxation experimental data. The study of the height and width parameters (a and b) showed that the relaxation time distribution function was nearly symmetric and close to the ideal Debye function.

In the temperature range used for this study, there existed dipoles that came into resonance at temperatures different than those corresponding to the ε'' maximum (α relaxation). When the mean temperature was taken as that dividing the ε''–temperature curve into two parts of equal surface, the values obtained through the dynamic and isothermal experiments practically coincided. This mean temperature should be taken as the representative one, together with the value of the relaxation time obtained, at this temperature, from the H–N equation. All the studied parameters had different values that depended on whether they were calculated from values corresponding to the ε'' maximum or from the mean values calculated from the numerical integration of the ε''–temperature curves.

The authors are indebted to J. M. Pereña for his interesting suggestions and to TA Instruments for checking their measurements with its own experiments. The DEA 2970 TA dielectric analyzer was acquired with funds from Secretaria Xeral de Investigación e Desenvolvemento (Xunta de Galicia).

References

1. Bisdrup, W. W.; Sheppard, N. F., Jr.; Senturia, S. D. Polym Eng Sci 1986, 26, 358.
2. Choy, I.-C.; Plazek, D. J. J Polym Sci Part B: Polym Phys 1986, 24, 1303.
3. Pazos Pellín, M.; Núñez Regueira, L.; López Quintela, A.; Paseiro Losada, P.; Simal Gándara, J.; Paz Abuín, S. J Appl Polym Sci 1995, 55, 1507.
4. Núñez, L.; Fraga, F.; Castro, A.; Fraga, L. J Therm Anal 1998, 52, 1013.
5. Montserrat, S.; Gómez Ribelles, J. L.; Meseguer, J. M. Polymer 1998, 39, 3801.
6. Ochi, M.; Lesako, H.; Shimbo, M. Polymer 1985, 26, 457.
7. Brown, M. E. Handbook of Thermal Analysis and Calorimetry; Elsevier: Amsterdam, 1998; Vol. 1.
8. Ferry, J. D. Viscoelastic Properties of Polymers, 3rd ed.; Wiley: New York, 1980; p 6.
9. Coln, M. C. W.; Senturia, S. D. Proc Transducers 85, 1985, 118.
10. Turi, E. A. Thermal Characterization of Polymeric Materials; Academic: San Diego, 1997.
11. Hunt, B. J.; James, M. I. Polymer Characterisation; Blackie: London, 1993.
12. Sheppard, N. F., Jr.; Senturia, S. D. J Polym Sci Part B: Polym Phys 1989, 27, 753.
13. Senturia, S. D.; Sheppard, N. F. Dielectric Analysis of Thermoset Cure; Advances in Polymer Science 80; Springer-Verlag: Berlin, 1986.
14. Debye, P. Polar Molecules; Chemical Catalog: New York, 1929.
15. Hunt, B. J.; James, M. I. Polymer Characterisation; Blackie: London, 1993.
16. Cole, K. S.; Cole, R. H. J Chem Phys 1941, 9, 341.
17. Davidson, D. W.; Cole, R. H. J. Phys Chem 1951, 19, 1484.
18. Havriliak, S.; Negami, S. J. Polym Sci C 1966, 14, 99.
19. Havriliak, S.; Negami, S. J. Polymer 1967, 8, 161.
20. Vogel, H. Phys Z 1921, 22, 645.
21. Williams, M. L.; Landel, R. F.; Ferry, J. D. J Am Chem Soc 1955, 77, 3701.
22. Núñez, L.; Fraga, F.; Núñez, M. R.; Villanueva, M. J Appl Polym Sci 1998, 70, 1931.
23. Núñez, L.; Fraga, F.; Núñez, M. R.; Castro, A.; Fraga, L. J Appl Polym Sci 1998, 74, 2997.
24. Matsukawa, M.; Okabe, H.; Matsushige, K. J Appl Polym Sci 1993, 50, 67.
25. Ochi, M.; Lesazo, H.; Shimbo, M. Polymer 1985, 26, 457.
26. Núñez, L.; Fraga, F.; Castro, A.; Fraga, L. J Appl Polym Sci 1998, 52, 1013.